Mon. Not. R. Astron. Soc. **000**, 1–14 (2014) Printed 15 July 2014 (MN LATEX style file v2.2)

The Mass Dependence of Satellite Quenching in Milky Way-like Halos

John I. Phillips,[1⋆] Coral Wheeler,[1] Michael C. Cooper,[1] Michael Boylan-Kolchin,[2] James S. Bullock,[1] Erik Tollerud[3]†
[1] *Center for Cosmology, Department of Physics and Astronomy, 4129 Reines Hall, University of California, Irvine, CA 92697, USA*
[2] *Astronomy Department, University of Maryland College Park, MD 20742-2421*
[3] *Astronomy Department, Yale University, P.O. Box 208101, New Haven, CT 06510, USA*

15 July 2014

ABSTRACT
Using the Sloan Digital Sky Survey, we examine the quenching of satellite galaxies around isolated Milky Way-like hosts in the local Universe. We find that the efficiency of satellite quenching around isolated galaxies is low and roughly constant over two orders of magnitude in satellite stellar mass ($M_\star = 10^{8.5} - 10^{10.5}\,M_\odot$), with only $\sim$ 20% of systems quenched as a result of environmental processes. While largely independent of satellite stellar mass, satellite quenching does exhibit clear dependence on the properties of the host. We show that satellites of passive hosts are substantially more likely to be quenched than those of star-forming hosts, and we present evidence that more massive halos quench their satellites more efficiently. These results extend trends seen previously in more massive host halos and for higher satellite masses. Taken together, it appears that galaxies with stellar masses larger than about 10^8 $M_\odot$ are uniformly resistant to environmental quenching, with the relative harshness of the host environment likely serving as the primary driver of satellite quenching. At lower stellar masses ($< 10^8$ $M_\odot$), however, observations of the Local Group suggest that the vast majority of satellite galaxies are quenched, potentially pointing towards a characteristic satellite mass scale below which quenching efficiency increases dramatically.

Key words: galaxies: formation – galaxies: evolution – galaxies: dwarf – galaxies: statistics – galaxies: star formation

1 INTRODUCTION

It is well documented that galaxy properties, such as morphology and star-formation rate, depend upon the local galaxy density, often referred to as the "environment" in which a galaxy is located. For instance, passive systems are systematically overrepresented in high-density environments at both low and intermediate redshift (e.g. Davis & Geller 1976; Dressler 1980; Lewis et al. 2002; Balogh et al. 2004; Hogg et al. 2004; Cooper et al. 2006, 2007, 2008, 2010a,b). This observed dependence of galaxy properties on local environment is most apparent at lower stellar masses, with satellite galaxies in groups and clusters exhibiting redder rest-frame colors, more bulge-dominated morphologies, as well as older and more metal-rich stellar populations than their counterparts of equal stellar mass in the field (e.g. Baldry et al. 2006; Yang et al. 2007; van den Bosch et al. 2008; Peng et al. 2010; Pasquali et al. 2010; Woo et al. 2013).

A variety of physical mechanisms are potentially responsible for the generally lower star-formation rates and higher incidence of bulges for satellite galaxies relative to their field counterparts. In particular, processes such as strangulation (Larson, Tinsley & Caldwell 1980; Balogh, Navarro & Morris 2000; Balogh & Morris 2000), ram-pressure stripping (Gunn & Gott 1972; Quilis, Moore & Bower 2000), and harassment (Farouki & Shapiro 1981; Moore et al. 1996) may preferentially suppress star formation and transform the structure of satellite galaxies in more massive halos (i.e. higher-density environments). At present, our understanding of which mechanism(s) dominate(s) the evolution of low-mass satellite galaxies is woefully incomplete. For example, modern semi-analytic models of galaxy evolution dramatically overpredict the number of passive satellite galaxies in the local Universe (Kimm et al. 2009; Weinmann et al. 2010, 2012) and many hydrodynamical models fail to reproduce the low-mass end of the stellar mass function at $z \sim 0$ (Crain et al. 2009; Davé, Oppenheimer & Finlator 2011).

⋆ e-mail: johnip@uci.edu
† Hubble Fellow

Understanding the mass dependence of satellite quenching represents a critical step towards identifying the specific physical processes at play in driving the evolution of low-mass galaxies as a function of environment. Simple models of ram-pressure stripping and strangulation predict an increased efficiency at low mass, such that less-massive satellites should be more readily quenched by these processes. In addition, understanding the dependence of environmental effects on host mass is similarly fundamental, as more massive host halos are likely to harbor a hotter and denser circumgalactic medium that may more efficiently strip or strangulate infalling satellite systems. In a previous paper (Phillips et al. 2014, hereafter P14), we pointed out a significant trend in satellite galaxy quenching that may result from this dependence on host mass: passive Milky Way-mass galaxies quench their satellites whereas star forming Milky Way-mass galaxies do not. Specifically, for massive satellites (with $M_\star \sim 10^{10}$ $M_\odot$), *passive* $\sim L^*$ hosts quench roughly 30% of their infalling satellites, while the satellites of *star-forming* $\sim L^*$ hosts exhibit the same star-forming activity as a field sample with the same stellar mass distribution. Using stacked line-of-sight satellite kinematics to estimate the host halo mass for these systems suggests that this dichotomy in quenching may be partially related to larger dark matter halo masses for passive L^* hosts relative to their star-forming counterparts at $z \sim 0$.

In this work, we expand upon the analysis of P14 by examining trends in satellite quenching beyond the dichotomy in host star-formation activity, focusing on the mass dependence of satellite quenching for Milky Way-like hosts. In particular, we compare satellites with stellar masses of $10^{8.5} - 10^{10.5}$ $M_\odot$ around a carefully-selected sample of isolated L^* galaxies to field galaxies with equivalent stellar mass and/or specific star-formation rate (SSFR) that are the central galaxy in their respective dark matter halo. By focusing on isolated hosts, we are able to probe systems residing in dark matter halos comparable to that of our Milky Way (a few $\times$ 10^{12} $M_\odot$, Deason et al. 2012; Boylan-Kolchin et al. 2013; van der Marel et al. 2012), while eliminating the known effects of more massive halos and large-scale structure on satellites. As motivated by the now well-established bimodality of galaxies in color-versus-luminosity space (i.e. the red sequence and blue cloud) and the dichotomy of quenching for which we argue in P14, we will often separately consider trends where the central host galaxy is passive from those where the central galaxy is star-forming. By characterizing the mass dependence of satellite quenching, we aim to constrain the physical mechanisms dominating the evolution of satellite systems in Milky Way-like halos.

The paper is structured as follows: In Section 2, we describe our methodology for identifying Milky Way-like halos and describe the specific criteria applied to create our central/host and satellite samples as well as our control samples. In Section 3, we present our primary findings on the dependence of satellite quenching efficiency on the properties of the satellite and host galaxies. Finally, in Section 4, we discuss the implication of the observed trends on galaxy formation models. Throughout our analysis, we employ a Λ cold dark matter (ΛCDM) cosmology with WMAP7+BAO+H0 parameters $\Omega_\Lambda = 0.73$, $\Omega_m = 0.27$, and $h = 0.70$ (Komatsu et al. 2011). Unless otherwise noted, all logarithms are base 10, and all quoted virial masses are derived from a spherical top-hat model according to the stellar mass/virial mass relation given in Guo et al. (2011).

2 SAMPLE SELECTION

In selecting our observational sample, we employ data from Data Release 7 (DR7) of the Sloan Digital Sky Survey (SDSS, York et al. 2000; Abazajian et al. 2009). In particular, we utilize the MPA-JHU derived data products, including median total stellar masses, photometrically derived according to Kauffmann et al. (2003, see also Salim et al. 2007), and median total star formation rates, measured from the SDSS spectra as detailed by Brinchmann et al. (2004). Spectroscopic completeness information as a function of position on the sky (i.e. *fgotmain*) is drawn from the NYU Value-Added Galaxy Catalog (NYU-VAGC, Blanton et al. 2005). Our selection criteria follow very closely those of P14, motivated by careful analysis of the Millennium II simulation (MS-II, Boylan-Kolchin et al. 2009). We will summarize them here; for a full discussion we refer the reader to that paper. Throughout this work, we refer to objects associated on the sky as "primaries" and "secondaries," while populations that have undergone correction for the presence of interlopers will be referred to as "hosts" and "satellites," as the corrected data more accurately reflect the properties of true host-satellite systems.

2.1 Sample Selection

For our sample of primaries, we select all objects in the SDSS spectroscopic sample with a stellar mass of $M_\star > 10^{10.5}$ $M_\odot$ and with $z < 0.032$, restricting to SDSS fiber plates with a spectroscopic completeness of >0.7 for the main galaxy sample. We then apply the following isolation criteria to preferentially select galaxies residing in halos of mass comparable to that of the Milky Way (a few $\times$ 10^{12} $M_\odot$), where the halo mass of host systems in our sample is calibrated by applying our selection criteria to the MS-II simulation. First, we allow no other galaxies with a stellar mass of $M_\star > 10^{10.5}$ $M_\odot$ within a cylinder defined by a radius of 350 kpc in projection and a length in velocity space of 2000 km s^{-1} along the line-of-sight and centered on the primary. In addition, we define an annulus with an inner (outer) radius of 350 kpc (1 Mpc), wherein we allow no more than one galaxy of stellar mass $M_\star > 10^{10.5}$ $M_\odot$. Galaxies that pass these criteria are deemed isolated primaries.

To select spectroscopically-confirmed satellites or secondaries around our isolated primaries, we define a search region with a radius of 350 kpc on the sky and $\pm$ 500 km s^{-1} in velocity space. We search for secondaries in two mass ranges: "massive secondaries" with stellar mass of $10^{9.5}$ $M_\odot < M_\star < 10^{10.5}$ $M_\odot$ and a maximum redshift of $z = 0.032$, and "dwarf secondaries" with stellar mass of $10^{8.5}$ $M_\odot < M_\star < 10^{9.5}$ $M_\odot$ and a maximum redshift of $z = 0.024$. These limiting redshifts are designed to ensure that we are complete at all stellar masses and SSFRs under consideration.

According to the number of massive secondaries identified about each primary, we divide our sample of isolated primaries, such that our main sample consists of primaries with exactly one secondary. As discussed by P14, restricting to systems with exactly one massive secondary in the SDSS

identifies halos with a mass distribution sharply peaked at a few $\times$ 10^{12} $M_\odot$. We also consider primaries with exactly zero and exactly two massive secondaries. However, primaries with three or more massive secondaries are excluded, since such systems are strongly biased towards the group/cluster regime. Figure 1 shows the virial mass distributions for primaries in our mass range from comparison to the MS-II simulation.[1] Applying our isolation criteria removes most primaries residing in clusters, while restricting the sample to primaries with at most two massive satellites strongly selects against systems with $M_{\rm vir} > 10^{13}$ $M_\odot$. Primaries with two massive satellites represent a subsample of isolated objects with greater virial masses, such that these systems are more likely to have $M_{\rm vir} \gtrsim 10^{12.4}$ $M_\odot$ than primaries with a single massive satellite. We give no consideration to the number of dwarf secondaries orbiting a primary.

For both of the secondary samples, we construct corresponding control samples of isolated field galaxies over the same mass and redshift ranges, which we will refer to as the "massive control" and "dwarf control" samples, respectively. These samples are subjected to an isolation procedure more rigorous than that of the primaries; for both samples, we require that no galaxy more massive than the lower mass limit of the respective sample be within 3 Mpc on the sky and $\pm$ 400 km s^{-1} in velocity. This ensures that the control samples are almost completely comprised of objects that are themselves the primary galaxy in their dark matter halo ($f_{\rm purity} \sim 97\%$, see P14 for a full discussion of purity considerations) — i.e. the samples are free of satellite galaxies. The number of objects in each of our samples, including control samples, is given in Table 1.

As shown in P14, there are dramatic differences in the effectiveness of quenching around passive and star-forming Milky Way-size hosts, such that only massive ($\sim$ 10^{10} $M_\odot$) satellites of passive Milky Way analogs are quenched relative to a stellar mass-matched sample of isolated field galaxies. Recognizing this dichotomy in satellite quenching, we divide our sample, including both primaries and secondaries, according to SSFR, with the division between passive and star-forming galaxies set to be

$$\log({\rm SSFR_{host}}) = -0.6\,\log({\rm M_\star}) - 5.2. \quad (1)$$

This equation is motivated by the established blue cloud/red sequence bimodality of galaxies in the SDSS (Strateva et al. 2001; Baldry et al. 2004). This passivity threshold matches the slope of the stellar mass-SSFR relation for star-forming galaxies in a self-consistent way. Figure 2 shows where our main and dwarf satellite samples reside in SSFR-stellar mass space, with the dividing line between passive and star-forming galaxies overplotted. We note that our qualitative results are not particularly dependent on our chosen division between star-forming and passive/quenched, such that other reasonable choices of quenching definition (e.g. a quenching threshold of SSFR $< 10^{-10.5}$ yr^{-1}) give similar results.

[1] For further details regarding the analysis of the MS-II simulation, we refer the reader to the detailed discussion in P14 as well as Section 2.2 herein.

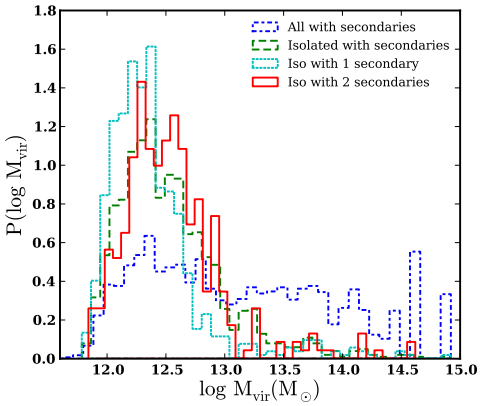

Figure 1. Virial mass distributions illustrating our host selection criteria. Shown are the virial mass distributions for all primaries with secondaries (blue short-dashed line), primaries that pass our isolation criteria and have at least one secondary (dashed green line), primaries that pass our isolation criteria and have exactly two secondaries (solid red line), and primaries that pass our isolation criteria and have exactly one secondary (dotted cyan line). Applying our selection criteria and restricting the number of massive satellites effectively removes massive halos from the sample. Primaries with fewer massive satellites tend to have lower virial masses. As shown by P14, restricting the sample to primaries with only one massive secondary efficiently selects Milky Way-like systems.

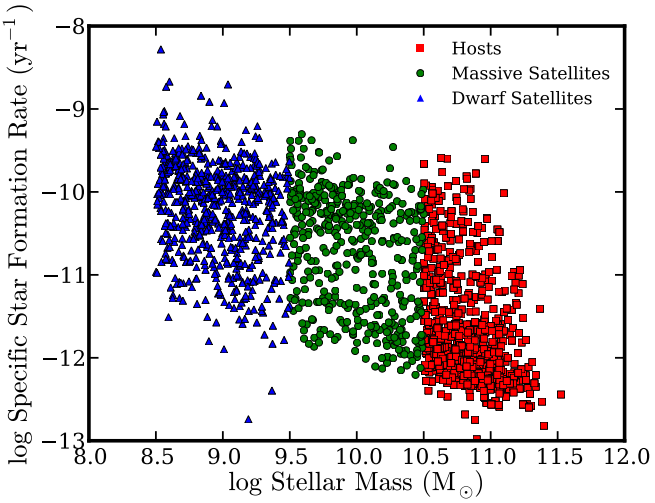

Figure 2. SSFR vs. stellar mass for our main sample. Plotted are all primaries at $z < 0.032$ and their massive ($10^{9.5}$ $M_\odot$ $< M_\star <$ $10^{10.5}$ $M_\odot$) secondaries. In our main sample, only primaries with exactly one massive secondary are considered. Also plotted is our dwarf ($10^{8.5}$ $M_\odot$ $< M_\star <$ $10^{9.5}$ $M_\odot$) secondary sample, which consists only of low-mass secondaries at $z < 0.024$. The dashed line separates objects into passive (below line) and star-forming (above line) categories.

2.2 Interloper Corrections and Parameter Matching

In this subsection, we discuss two numerical procedures employed to approximate the distributions of "true satellite" properties (rather than simply secondary properties) and to compare samples to corresponding control samples in a self-consistent way.

Mass Range	Sample	N	$< \log M_\star >$
Massive $10^{9.5} M_\odot < M_\star < 10^{10.5} M_\odot$	One Satellite ("Main Sample")	457	9.98
	Two Satellites	306	9.98
	Control	581	9.94
Dwarf $10^{8.5} M_\odot < M_\star < 10^{9.5} M_\odot$	Satellite	665	8.95
	Control	302	9.16

Table 1. Number of galaxies and mean log $M_\star$ in the satellite and control samples used in this study. Massive and dwarf satellites (along with their respective control samples) are restricted to stellar masses of $10^{9.5}$ $M_\odot < M_\star < 10^{10.5}$ $M_\odot$ and $10^{8.5}$ $M_\odot < M_\star < 10^{9.5}$ $M_\odot$, respectively.

In P14, we describe in detail how we connect observations to the dark-matter only Millennium II Simulation (Boylan-Kolchin et al. 2009). In short, we wish to use the simulations to disentangle objects that are truly bound to their hosts from objects that, despite having velocities that would suggest their being part of the system, are not. This requires two critical pieces of information: perfect phase-space information about the objects in question, which the simulations provide, and a functional model that links dark matter halos to galaxies in the real Universe. For the latter, we adopt the subhalo abundance matching (SHAM) prescription of Guo et al. (2011). While abundance matching has difficulty predicting the dark matter halo masses of the local dwarf galaxy population (Boylan-Kolchin, Bullock & Kaplinghat 2011, 2012; Garrison-Kimmel et al. 2014), it is very successful in reproducing the clustering of more massive galaxies, including the mass range probed by our work (Berrier et al. 2006; Conroy, Wechsler & Kravtsov 2006).

In order to ascertain the distributions and values of parameters for the true satellite population, we correct for the presence of interlopers statistically. This is done by taking the cumulative distribution of a given parameter in the secondary population and subtracting the distribution of the control sample multiplied by the probability that a randomly selected galaxy is an interloper (i.e. $1 - f_{\rm purity}$). The result is an unnormalized cumulative distribution of the parameter in the *satellite* population. We renormalize so as to produce a well behaved cumulative distribution function. The equation for the satellite distribution of a parameter, here F, is given by

$$F_{\rm satellite} = \frac{F_{\rm secondary} - (1 - f_{\rm purity}) F_{\rm control}}{f_{\rm purity}}. \quad (2)$$

Note that this requires the assumption that all "impurities" are isolated interlopers. To ease this assumption, we make the above calculation using a modified definition of $f_{\rm purity}$, where $f_{\rm purity}$ measures the fraction of secondaries in our sample that are satellites of any host, not necessarily the identified host.

Often, as in the case of comparisons between satellite and control samples, we wish to control for distributions of parameters correlated with those under investigation. For example, to control for mass dependencies, we match the stellar mass distributions of a given satellite subsample to a control sample by dividing both subsamples into bins in the relevant parameter (e.g. stellar mass). For each bin, we then randomly select, with replacement, an object from the second sample for each object in the first sample, yielding two samples of equal number that are matched on a given parameter. Whenever this is done, the process is repeated 100 times.

3 SATELLITE QUENCHING AS A FUNCTION OF SYSTEM PROPERTIES

In P14, we introduce a parameter to quantify quenching efficiency: the conversion fraction ($f_{\rm convert}$), which is defined as the difference in the quenched fraction between the satellite and control samples relative to the unquenched fraction of the control sample. In other words, let the unquenched fraction $u_{\{\rm sat,control\}}(\log {\rm SSFR} = X)$ equal the fraction of satellites or control galaxies with $\log {\rm SSFR} > X$, and the quenched fraction $q_{\{\rm sat,control\}}(\log {\rm SSFR} = X) = 1 - u_{\{\rm sat,control\}}$ be the fraction of satellites or control galaxies with $\log {\rm SSFR} < X$. The conversion fraction, $f_{\rm convert}$, is then given by

$$f_{\rm convert} = \frac{q_{\rm sat} - q_{\rm control}}{u_{\rm control}}. \quad (3)$$

In short, $f_{\rm convert}$ corresponds to the fraction of star-forming galaxies that have been quenched upon infall onto the halos of a given set of hosts. This relies on the assumption that the properties of the control sample are adequately representative of the properties of the progenitors of the satellite samples, which is not a perfect assumption. Most satellites are star-forming, such that they continue to increase their stellar masses over time, even though they fell onto a host some time in the past. Other works have used a similar statistic to our conversion fraction, including van den Bosch et al. (2008) and Peng et al. (2012).

Throughout this analysis, errors on the quenched fractions are computed according to binomial statistics as

$$\sigma_{\rm q,sample} = \sqrt{\frac{(q_{\rm sample})(1 - q_{\rm sample})}{N_{\rm sample}}}, \quad (4)$$

where $\sigma_{\rm q,sample}$ is the error on the quenched fraction of the sample, $q_{\rm sample}$ is the quenched fraction of the sample, and $N_{\rm sample}$ is the number of objects in the sample. These errors are then propagated according to Equation 3 to determine the associated errors on the conversion fractions.

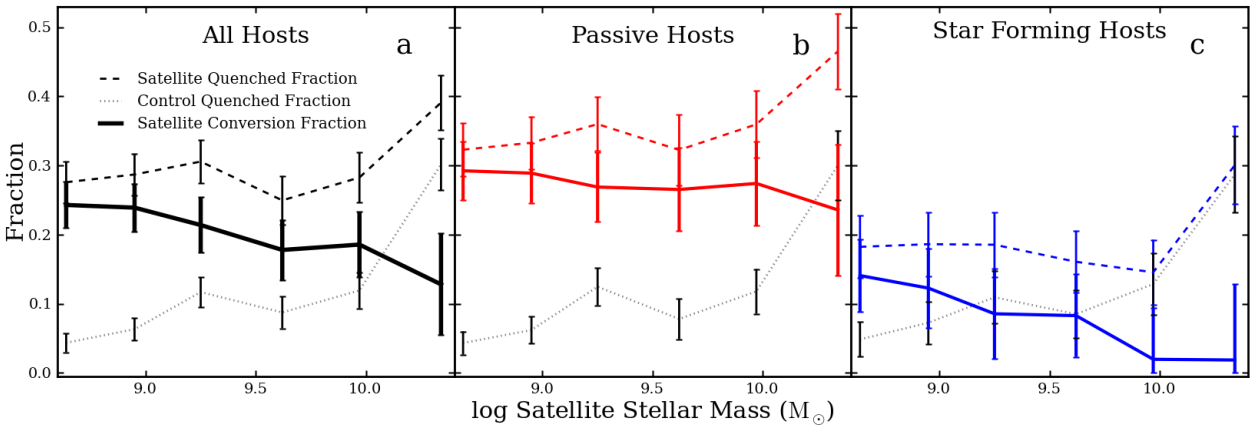

Figure 3. The conversion fraction for satellites of all hosts (*left panel*), passive hosts (*center panel*), and star-forming hosts (*right panel*) as a function of satellite stellar mass in our main sample (*solid lines*). For reference, the quenched fraction for the respective satellite samples (*dashed lines*) and mass-matched control samples (*dotted lines*) are also shown. The conversion fraction is independent of stellar mass in the passive host sample, while exhibiting a negative correlation with satellite mass in the star-forming host sample, such that less-massive satellites of star-forming hosts are more likely to be quenched upon infall.

3.1 Dependence on Satellite Mass

Considering both our main and dwarf subsamples, our full sample of satellite galaxies spans two orders of magnitude in stellar mass, $10^{8.5} < M_\star/M_\odot < 10^{10.5}$. To explore the dependence of quenching on stellar mass, we separate our satellite sample into six distinct bins, by independently dividing the main and dwarf subsamples according to the 33rd and 67th percentiles in stellar mass. The resulting six independent bins are bounded in stellar mass space by $10^{8.5}$, $10^{8.80}$, $10^{9.11}$, $10^{9.5}$, $10^{9.79}$, $10^{10.14}$, and $10^{10.5}$ $M_\odot$. In Figure 3a, we show the passive fraction for the satellite samples in each stellar mass bin (dashed line) along side that of the control samples of isolated galaxies (dotted line) with the same stellar mass distribution (i.e. "mass-matched"). As highlighted by previous studies of satellite galaxies in the local Universe, predominantly in more-massive halos, we find that satellites are preferentially passive relative to the field population (e.g. Weinmann et al. 2006; Tollerud et al. 2011; Geha et al. 2012; Wang & White 2012).

Following Equation 3, the measured passive fractions for the satellite and control samples yield a conversion fraction as a function of satellite mass that weakly increases with decreasing stellar mass, such that less-massive satellites are slightly more likely to be quenched upon infall to a Milky Way-like halo (see solid line in Fig. 3a). Within the errors, however, the measured conversion fractions are largely consistent with no dependence on satellite stellar mass at $10^{8.5}$ $M_\odot < M_\star < 10^{10.5}$ $M_\odot$. Using repeated Monte Carlo resampling and assuming the stated errors are normally distributed,[2] we estimate the slope of the relation between conversion fraction and $\log M_\star$ to be -0.069 ± 0.036, marginally inconsistant with no correlation and consistent with a slight anti-correlation.

As shown by P14, the conversion fraction (and thus efficiency of satellite quenching) varies significantly between passive and star-forming Milky Way-like hosts, such that massive ($\sim 10^{10}$ $M_\odot$) satellites are only quenched around passive hosts. Given this observed dichotomy of massive satellite quenching, we compute the passive and conversion fractions as a function of satellite stellar mass for passive and star-forming hosts separately (see Figure 3b,c). At all satellite stellar masses probed, passive hosts are more effective at quenching than star-forming hosts. Moreover, we again find that at high satellite masses, passive hosts are the sole drivers of satellite quenching, with a conversion fraction for satellites of passive hosts of roughly 30% relative to nearly 0% around star-forming systems. Remarkably, across the entire range of satellite stellar masses studied, this moderate quenching efficiency (of $\sim 30\%$) is relatively independent of satellite mass for passive hosts. Using the Monte Carlo method described above, we find a slope in the conversion fraction-satellite stellar mass relation of -0.027 ± 0.048, consistent with no dependence of quenching efficiency on satellite stellar mass for passive Milky Way-like hosts. Conversely, we find weak evidence for a modest increase in the conversion fraction at lower stellar masses around star-forming systems, with a slope of -0.089 ± 0.058. This suggests that the weak negative slope seen with passive and star forming hosts taken together is driven by the anti-correlation in quenching efficiency and satellite stellar mass found around star-forming hosts.

3.2 Dependence on Host Mass

It is natural to expect that the efficiency of satellite quenching correlates with the stellar mass of the host. For example, galaxies of higher stellar mass tend to live in more massive dark matter halos (Mandelbaum et al. 2006; Conroy et al. 2007; Behroozi, Wechsler & Conroy 2012; McGaugh 2012; Moster, Naab & White 2013; Miller et al. 2011, 2014), which may quench satellites more effectively. This trend is observed on large scales, with clusters hosting significantly higher fractions of passive galaxies relative to comparable field samples (e.g. Dressler 1980; Postman et al. 2005). With this thought in mind, we study the dependence of quenching efficiency on host stellar mass within our sample of less-

[2] Our samples are large enough that the assumption of normally-distributed errors is valid, typically on the order of n = 60 - 100.

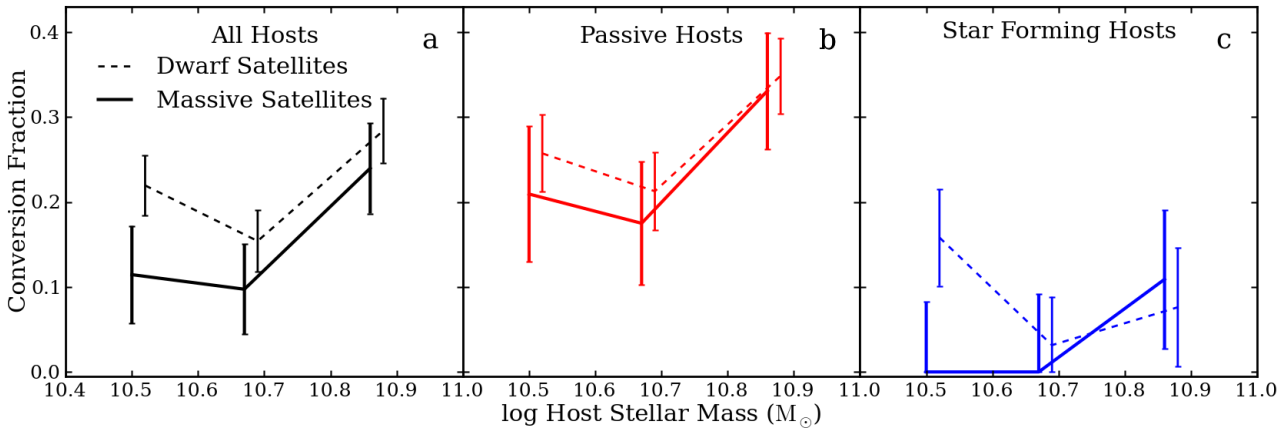

Figure 4. Conversion fractions for satellites in our main sample (*solid lines*) and dwarf sample (*dashed lines*) as a function of the stellar mass of their host, divided according to the star-forming properties of the host. Left panel: all hosts, center panel: passive hosts, right panel: star-forming hosts. We find little evidence for a dependence of satellite quenching effiency on host stellar mass.

extreme, lower-mass halos. Hosts are divided into three mass bins bounded by the 33$^{\rm rd}$ and 67$^{\rm th}$ percentiles of the host stellar mass distribution, which correspond to stellar masses of $10^{10.69}$ M$_\odot$ and $10^{10.86}$ M$_\odot$, respectively.

To examine how quenching efficiency depends on the stellar mass of the host, we examine the satellites in the main and dwarf sample separately, as shown in Figure 4, and divide the hosts according to their status as passive or star-forming. This gives us four independent subcategories that we can use to examine the host stellar mass dependence of quenching efficiency: massive satellites of passive hosts, massive satellites of star-forming hosts, dwarf satellites of passive hosts, and dwarf satellites of star-forming hosts. Of the four subsamples, all but the dwarf satellites of star-forming hosts exhibit a similar correlation between f$_{\rm convert}$ and host stellar mass: constant quenching efficiency in the two lower host mass bins, with a slight increase in quenching efficiency in the highest mass bin. We again use Monte Carlo resampling to test whether the slope of the conversion fraction-host stellar mass relation is consistent with zero in each subsample — that is, wether or not the increase in quenching efficiency at high host stellar mass is statistically significant. In all cases, we find that the observed quenched efficiencies are largely consistent with no dependence on host mass, such that the measured slopes of the conversion fraction versus log(M$_\star$) relation are consistent with zero at $< 2\sigma$.

The subsample that differs significantly from the other three categories, dwarf satellites of star-forming hosts, sees an increase in quenching efficiency around the lowest mass hosts. We showed in the previous subsection that lower mass satellites of star-forming hosts are more likely to be quenched; however, the increase in the efficiency with which dwarf satellites are quenched in low-mass star-forming hosts is likely not driven by an decrease in the characteristic stellar mass of satellites of such hosts. A Kolmogorov-Smirnov (KS) test fails to show that the stellar masses of the objects in the three dwarf satellite/star-forming host bins are drawn from different underlying distributions ($p_{lower,middle} = 0.71$, $p_{lower,upper} = 0.37$). While the behavior of dwarf satellites of star-forming galaxies does seem odd, the data are consistent with no dependance in conversion fraction on host stellar mass.

3.3 Dependence on Satellite Number

As discussed in §2, we have to this point restricted our analysis to hosts with exactly one massive satellite, as this preferentially selects Milky Way-like systems in lieu of more massive dark matter halos (see Fig. 1). Here, we relax this restriction on the number of massive satellites and consider separately hosts that have exactly one massive satellite and hosts with more than one massive satellite. These categories represent hosts with different characteristic virial masses. As shown in Fig. 1, we find that hosts with two massive satellites live in systematically more massive dark matter halos based on comparison to the MS-II simulation.[3] For ease of comparison with P14, we adopt a simplified threshold for quenching, by which satellites will be considered quenched if their SSFR is below 10^{-11} yr^{-1}. In Figure 5, we plot the cumulative distribution of specific star formation rates for massive satellites around passive and star-forming hosts separately, matching the stellar mass distributions of all four host samples. For hosts with only one massive satellite, the dichotomy of quenching discovered in P14 is readily apparent, with satellites of passive hosts more than twice as likely to be quenched than a stellar mass-matched field sample and satellites of star-forming hosts indistinguishable from their field counterparts. For systems with multiple massive satellites, however, the behavior is different. Passive hosts with two satellites still quench their satellites more efficiently than star-forming hosts with two satellites, but star-forming hosts now exhibit non-zero quenching efficiency, possibly pointing to a trend in quenching efficiency with host halo mass.

In light of the evidence that more massive halos quench their satellites more effectively, we might hypothesize that there exists a critical halo mass threshold above which a host

[3] The median halo mass for isolated hosts with two massive secondaries is approximately 60% larger than that for isolated systems with only one massive secondary in the MS-II simulation.

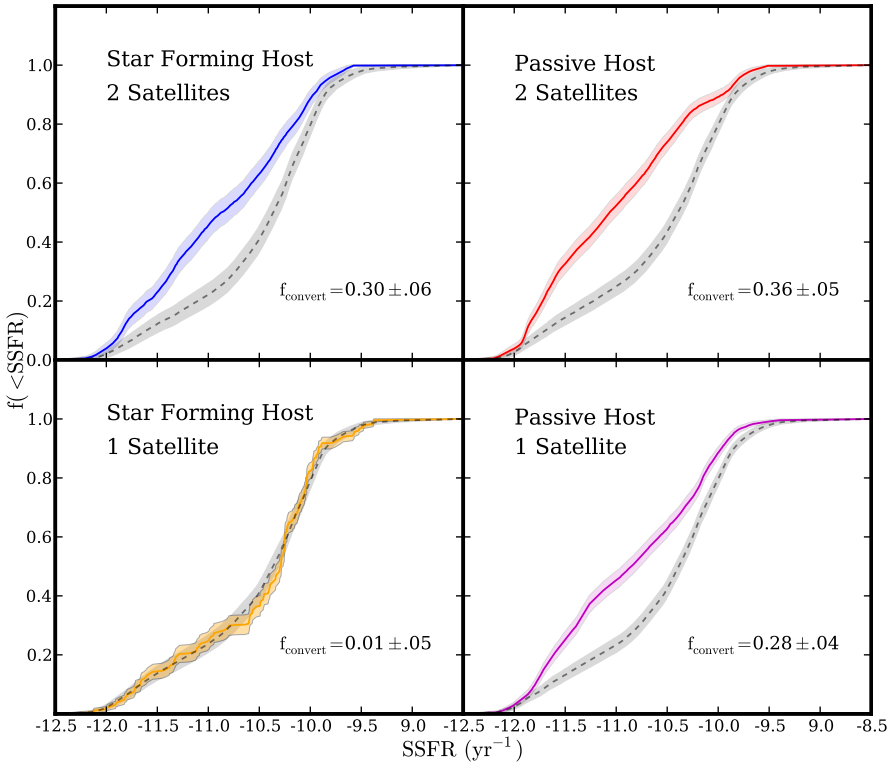

Figure 5. Cumulative distributions of specific star formation rate for massive satellites of passive (right column) and star-forming (left column) hosts with exactly one (bottom row) and exactly two (top row) satellites. The black dashed lines show the corresponding distributions for stellar mass-matched samples of isolated field galaxies. Colored and grey shaded regions correspond to 1σ binomial errors for the satellite and control samples, respectively. Hosts with two massive satellites are more effective at quenching those satellites than corresponding hosts with only one satellite, and star-forming hosts with two satellites have a non-zero quenching efficiency, breaking the dichotomy of quenching presented in P14.

will quench its satellites extremely efficiently. This could be considered a potential limiting case of quenching scenarios, whereby in a two-satellite system the conditional probability of finding a satellite quenched given that its partner is quenched is near unity. An alternate limiting case might be that the probabilities of finding either satellite quenched are independent of each other. How well the data conform to either limiting case can inform quenching models, and by examining our sample host-by-host, we can examine how the satellites are distributed among the hosts.

Considering each two-satellite system individually, we ask whether the satellites are matched or unmatched in their star-forming properties. Figure 6 shows the frequency of passive, star-forming, and mis-matched satellite pairs around passive and star-forming hosts. For comparison, we also plot the binomial distributions for both samples — i.e. the expectation from randomly drawing satellites from the population of all satellites. In the observational sample, mis-matched pairs are better represented than the matched pairs of passive or star-forming satellites. While the incidence of mismatched pairs is lower than the binomial distribution and the frequencies of matched passive and star-forming pairs are higher than the binomial distribution, the disagreement is fairly minor. For a system with two massive satellites, having one satellite be passive corresponds to a slightly higher probability of its partner being passive and vice versa for star-forming satellites. We note that the distributions are very similar between the two host types, and despite statistically signifiant deviation from the binomial distribution, the distribution of observed pairs is much better modeled by a binomial distribution than the limiting case of all satellites being found in matched pairs.

Satellite galactocentric distance can provide information about the environment in which it lives, such as what type of CGM it is embedded in or how long it has been interacting with its host. With that in mind, we examine the projected distance distribution of satellite galaxies in systems with exactly two massive satellites. In Figure 7, we examine the radial distribution of satellites in systems with two massive satellite, grouping the satellites according to their star-forming properties as well as that of the host. The top and bottom sets of three panels show the distributions for satellites of passive and star-forming hosts, respectively.

Of particular interest is the difference between the radial distributions of passive satellites compared to their star-forming counterparts. We find that passive satellites are more likely to be found at small projected radii, while there is a corresponding overabundance of star-forming satellites in the outer regions of the halo. This trend is apparent in the mixed satellite cases, and is readily seen upon comparing passive and star-forming satellites across the various host subsamples. A Kolmogorov-Smirnov (KS) test rejects the null hypothesis that the distributions of projected distances are identical between star-forming and passive satel-

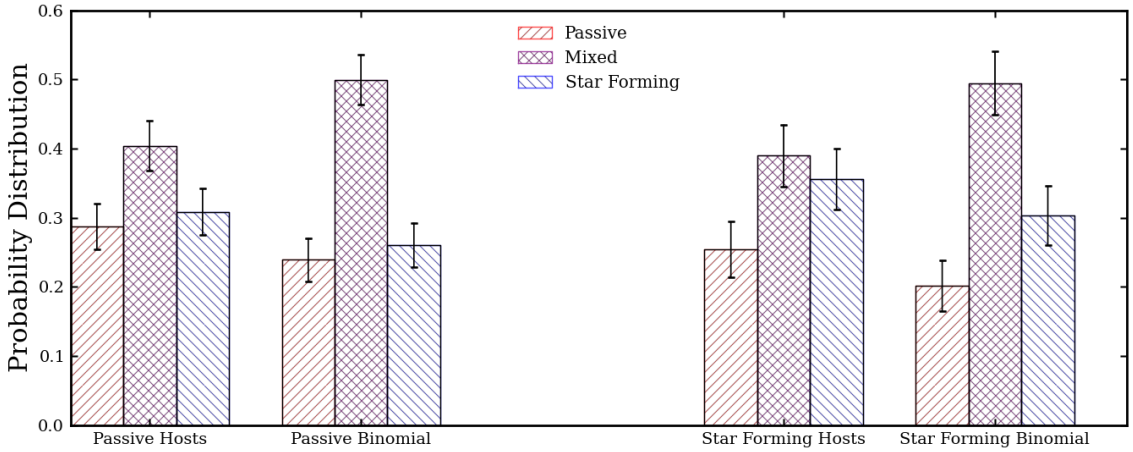

Figure 6. The relative frequency of matched or mis-matched satellite properties in two satellite systems for passive (*left*) and star-forming (*right*) hosts. Shown separately are the frequency of matched passive pairs (red bars), matched star-forming pairs (blue bars) and mixed pairs (i.e. one passive satellite and one star-forming satellite, purple bars). Also plotted are binomial distributions calculated from the red fraction of satellites in the parent passive and star-forming host categories, representative of the limiting case where satellites are randomly assigned to hosts. In systems with two satellites, having one passive satellite corresponds to a slightlyhigher likelihood of the second satellite also being passive and vice versa for star-forming satellites.

lites ($p = 0.004$). This trend is particularly apparent in the cases where one satellite is star-forming and one satellite is passive (middle panels of Fig. 7); for both passive and star-forming hosts, the star-forming satellites are more likely to be found in the outer regions of the host halo relative to the passive satellites.

The one category that seems not to follow the trend is the category of star-forming hosts with paired passive satellites. Here we find, despite low statistics, that satellites are mostly found at large projected distances. One possible interpretation of this result is that a relatively high portion of these objects were not environmentally quenched by their host, but rather quenched in the field. We might expect that if the satellites had been environmentally quenched at a similar rate to the other categories, they would be found at projected distances more in line with those seen in the other categories. Alternately, the apparent inversion of the radial trend seen in the other subsamples could be the result of host misidentification. In situations where the hosts and satellites have a nearly one-to-one mass ratio, if the true host of the system is misidentified as a distant satellite, the unexpected case of a host having a distant passive satellite would indeed be the expected case of a host having a distant star-forming satellite. Of the 30 objects identified as satellites in this subsample, 12 have projected distances greater than 250 kpc. Of these, 5 are within a factor of three of their host in stellar mass, comprising 4 of the 15 systems. If these four systems are disregarded, the radial distribution of passive satellites becomes flat, more in line with the other subsamples of passive galaxies.

4 DISCUSSION

In this paper, we have examined the dependence of satellite quenching on the mass of the satellite galaxy, the mass of the host galaxy, and the multiplicity of satellites in the system. For our host and satellite sample, we show that satellite quenching is not strongly correlated with satellite mass and potentially increases with increasing host virial mass, as best shown by an increase in conversion fraction in systems with two massive satellites. We also demonstrate that within such systems, passive and star-forming satellites are found around hosts roughly with frequencies described by a binomial distribution, implying little correlation between the properties of satellite pairs. In the following section, we discuss these results in comparison to previous studies in the local Universe and highlight the implications of these findings on models of galaxy evolution.

4.1 The Mass Dependence of Satellite Quenching

Across a broad range in stellar mass, $10^{8.5}$ $M_\odot$ $< M_\star <$ $10^{10.5}$ $M_\odot$, we find little evidence for a correlation between conversion fraction (i.e. the efficiency of satellite quenching) and satellite stellar mass, with Milky Way-like hosts quenching $\sim$ 20% of infalling satellites on average. This relatively inefficient quenching is strongly correlated with host properties, such that the satellites of passive hosts, at all masses probed, are more likely to be quenched than their counterparts around star-forming hosts. Moreover, for the most massive satellites ($\sim$ 10^{10} $M_\odot$), quenching is entirely driven by the halos of passive hosts, with massive satellites of star-forming hosts indistinguishable from the field population — a confirmation of the dichotomy of satellite quenching shown in P14. At lower satellite stellar masses ($\sim$ $10^{8.5}$ $M_\odot$), however, we measure a conversion fraction of $\sim$ 15% for satellites of star-forming hosts. This breaks the strong dichotomy of satellite quenching observed at higher masses, though the mass dependance of satellite quenching efficiency for satellites of star-forming hosts is mild.

The lack of significant correlation between satellite stel-

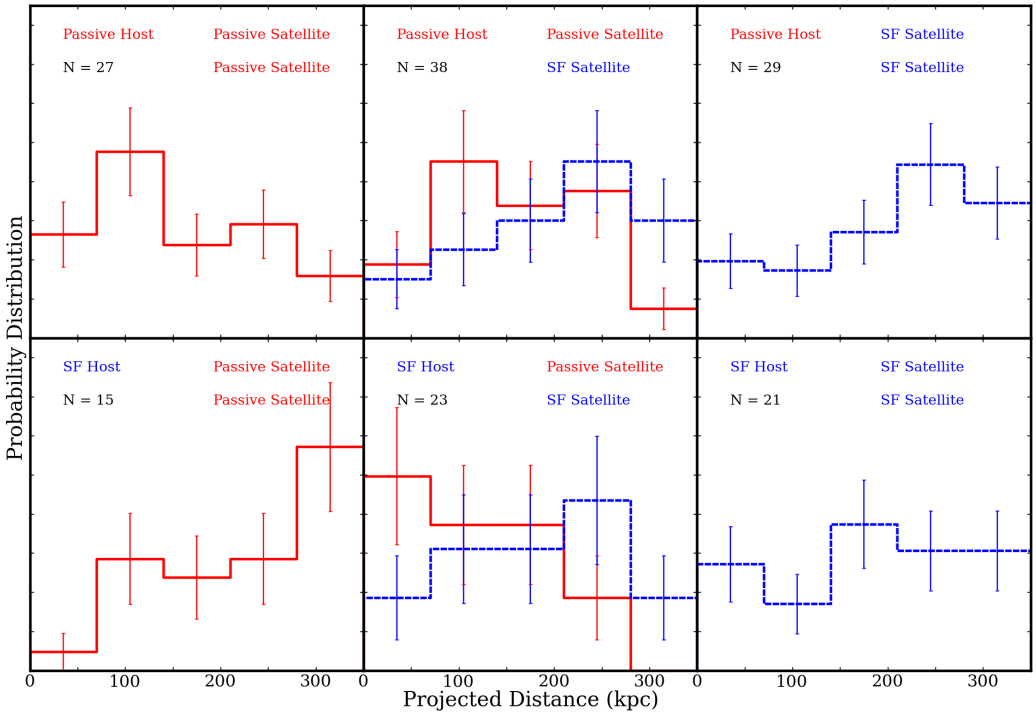

Figure 7. Radial distributions of massive satellites for passive (*top row*) and star-forming (*bottom row*) hosts with exactly two massive satellites. In each row, we divide the subsamples into passive satellite pairs (*left column*), mixed satellite pairs (*center column*), and star-forming satellite pairs (*right column*). In each case, passive satellite distributions are represented by a solid red line and star-forming satellite distributions by a dashed blue line. There is an overall trend for passive satellites to be more centrally concentrated than their star-forming counterparts. The overabundance of passive satellites at large projected distances in the bottom left panel may be a result of mis-identifying the host galaxy.

lar mass and conversion fraction is surprising. In accordance with subhalo abundance matching, lower stellar mass galaxies tend to occupy lower virial mass (and thus less dense) halos. Given their shallower potential wells, these galaxies would therefore be expected to lose their gas more easily and become quenched, thereby yielding a higher conversion fraction at lower satellite masses. However, this is not observed.

One possibility is that the expected trend for low-mass galaxies to lose their gas (and thus quench) more easily may be balanced out by a tendency for these systems to possess larger gas reservoirs. Under a scenario where hot gas is stripped from a satellite upon infall but cold gas is retained (i.e. "strangulation"), galaxies with higher cold gas fractions would thereby take longer to use up their gas and ultimately quench. According to observations of atomic hydrogen in local star-forming galaxies, lower stellar mass systems are generally found to have higher atomic gas fractions and longer atomic depletion timescales (SFR/M_{HI}) than their more massive counterparts (Skillman, Côté & Miller 2003; Geha et al. 2006; Leroy et al. 2008; Schiminovich et al. 2010). Furthermore, recent studies of molecular gas, which more closely traces ongoing star formation (Wong & Blitz 2002; Kennicutt et al. 2007; Bigiel et al. 2008), also show increasing cold gas fractions at lower stellar masses (Saintonge et al. 2011; Boselli et al. 2014). Altogether, the overall trend for the progenitors of low-mass satellite to have high cold gas fractions and correspondingly long depletion times may serve to counteract the tendency for low-mass satellites to lose gas easily, resulting in an overall non-dependence of conversion fraction on satellite stellar mass. While the efficiency of satellite quenching is observed to be relatively independent of satellite stellar mass, we do find a significant increase in the conversion fraction, $f_{convert}$, with increasing host halo mass. In particular, we find a greater satellite quenching efficiency for host systems with two massive satellites relative to those with only one massive satellite (see Fig. 5), where comparison to the MS-II simulation shows that systems with more massive satellites are preferentially biased towards greater dark matter virial masses (see Fig. 1). Our measurements of stacked satellite velocity dispersions confirm that hosts with two massive satellites preferentially reside in more massive halos. As in P14, we stack the line-of-sight velocity distributions for satellites of passive and star-forming hosts at fixed host stellar mass, so as to measure the velocity dispersion as a proxy for the characteristic virial mass of the respective host populations. Passive hosts with one satellite have a satellite velocity dispersion of 165 ± 11 km s^{-1}, while passive hosts with two satellites have a satellite velocity dispersion of 197 ± 13 km s^{-1}, such that passive hosts with two satellites live in more massive dark matter halos than passive hosts with one satellite. Likewise, star-forming hosts with a single massive satellite yield a stacked satellite velocity dispersion of 148 ± 14 km s^{-1}, whereas star-forming hosts with two massive satellites have a satellite velocity dispersion of 189 ± 16 km s^{-1}, implying the same about star-forming hosts.

The apparent correlation between satellite quenching efficiency and host halo mass may also explain the increased

prevalence of quenched satellites around passive hosts relative to their star-forming counterparts. As shown in Fig. 5, the conversion fraction for satellites of passive Milky Way-like hosts, in both the one- and two-satellite cases, exceeds that measured for satellites of star-forming hosts (see also Fig. 3). The comparison of stacked satellite velocity dispersions for these samples shows that even at fixed satellite number, as well as fixed stellar mass, passive hosts preferentially live in more massive dark matter halos. Thus, as discussed by P14, a quenching efficiency that depends on host halo mass in concert with the preference for passive hosts — at a given stellar mass — to reside in more massive halos directly explains the increased prevalence of quenched satellites around passive hosts.

Beyond dynamical tracers of halo mass, host stellar mass is also expected to track halo mass on average, with more massive host galaxies typically residing in more massive halos (e.g. Moster et al. 2010; Miller et al. 2014). Yet, while we do find mild evidence for an increase in quenching efficiency at high host stellar mass, our results are largely consistent with no correlation between conversion fraction and the stellar mass of the host. One possible explanation for this lack of observed correlation between satellite quenching and host stellar mass is that our sample spans a relatively narrow range in host stellar mass, such that we cannot resolve a clear stellar mass-halo mass relation — i.e. the stellar mass-halo mass relation may be largely dominated by scatter over the range in halo masses probed by our hosts. To test this possibility, we again stack the satellites of the hosts in each host stellar mass bin and measure the velocity dispersions of the massive satellite populations. We find no trend in satellite velocity dispersion with increasing host stellar mass: the lowest bin in host stellar mass has a velocity dispersion of 163 ± 10 km s^{-1}, the middle bin has a velocity dispersion of 162 ± 11 km s^{-1} and the upper bin has a velocity dispersion of 155 ± 9 km s^{-1}. This suggests that the evidence we find for a strong dependence of quenching efficiency on host halo mass and for weak to no dependence of quenching efficiency on host stellar mass do not necessarily contradict each other and are consistent with a picture where higher virial mass hosts are more likely to quench their satellites.

As discussed in P14, the dependence of quenching efficiency on host halo mass may reflect the preference for more massive dark matter halos to harbor hot gas coronas, which are then able to quench infalling satellite galaxies via ram-pressure stripping. Studies of gas accretion onto dark matter halos indicate that there is a transition in the dominant accretion mode at a halo mass of roughly a few $\times 10^{12}$ M$_\odot$. Infalling gas is shock-heated at the virial radius in halos above this threshold, while cold gas reaches a smaller radius, possibly falling all the way to the galaxy, in less-massive halos (e.g. Binney 1977; Rees & Ostriker 1977; Birnboim & Dekel 2003; Kereš et al. 2005, 2009; Stewart et al. 2011). Models of galaxy formation in which quenching only occurs above this critical halo mass show significant promise in reproducing the observed dependence of the galaxy quenched fraction on stellar mass and environment at $> 10^{9.5}$ M$_\odot$ (Gabor & Davé 2014). Our results, as presented in Fig. 5, are largely consistent with this picture of gas accretion and stripping, such that star-forming hosts with one massive satellite preferentially reside in halos below the critical halo mass and passive hosts with one massive satellite as well as all hosts with two massive satellites inhabit more massive halos with established hot coronas. In the less massive halos, the satellite galaxies largely mirror the field population, while roughly 30% of infalling satellites are quenched in more massive systems, potentially due to the presence of a hot halo.

It should be noted, however, that models such as these, which depend on interactions with host circumgalactic media to drive satellite quenching, may struggle to reproduce the observed correlation between the star-forming properties of massive galaxies and that of lower-mass systems located at distances of several virial radii (e.g. Kauffmann et al. 2013; Wetzel et al. 2014). Alternatively, work by Hearin, Watson & van den Bosch (2014) presents a picture where the importance of intra-halo quenching mechanisms is overstated, and large scale conformity, i.e. two-halo effects, is important.

While clear evidence is found for a correlation between quenching efficiency and halo mass, the observations of two-satellite systems are not – at first glance – entirely consistent with this picture. As shown in Fig. 6, the star-forming properties of satellites are consistent with being randomly drawn from the parent population, such that if one massive satellite is quenched in a system then the second satellite is only marginally more likely to also be quenched. In a scenario where quenching is driven entirely by host halo mass, one might expect that quenched satellites would be preferentially found within a particular subset of halos (e.g. within those more massive halos with a CGM capable of stripping an infalling satellite). This reasoning, however, assumes that satellites quench on a reasonably short timescale, such that there is a relatively small chance of observing a star-forming satellite within a halo capable of quenching it. Recent studies of quenching timescales for low-mass satellites suggest that this assumption is flawed, with satellites with a stellar mass of $\sim 10^{10}$ M$_\odot$ estimated to quench ~ 6 Gyr after infall (De Lucia et al. 2012; Wetzel et al. 2013; Wheeler et al. 2014). Adopting this quenching timescale within the MS-II simulation, where infall times are known, and assuming that all systems with two massive satellites are above the critical halo mass, we are able to precisely reproduce the distributions of matched and mis-matched satellite pairs shown in Figure 6, under the assumption that only subhalos accreted more than 5 Gyr ago are quenched. Additional models could potentially be constrained with quenching timescales that vary with host mass and a critical halo mass above which a host can quench and below which it can not.

4.2 Comparison to Previous Studies

Using data drawn from the SDSS, several recent studies similarly conclude that satellite quenching efficiency is largely independent of satellite stellar mass at $10^8 \lesssim$ M$_\star$/M$_\odot$ $\lesssim 10^{11}$ (Geha et al. 2012; Wetzel et al. 2013; Wheeler et al. 2014). In particular, Wetzel et al. (2013) employ the group catalog of Yang et al. (2005, 2007) to study the frequency of quenched satellites at $> 10^{9.7}$ M$_\odot$, showing that $\sim 30\%$ of massive satellites are quenched upon infall to a host halo. Using the data of Geha et al. (2012) to push to lower satellite masses, Wheeler et al. (2014) extend this work by studying the quenching efficiency around local hosts with stellar masses of $> 10^{10.4}$ M$_\odot$, finding a comparable quenching ef-

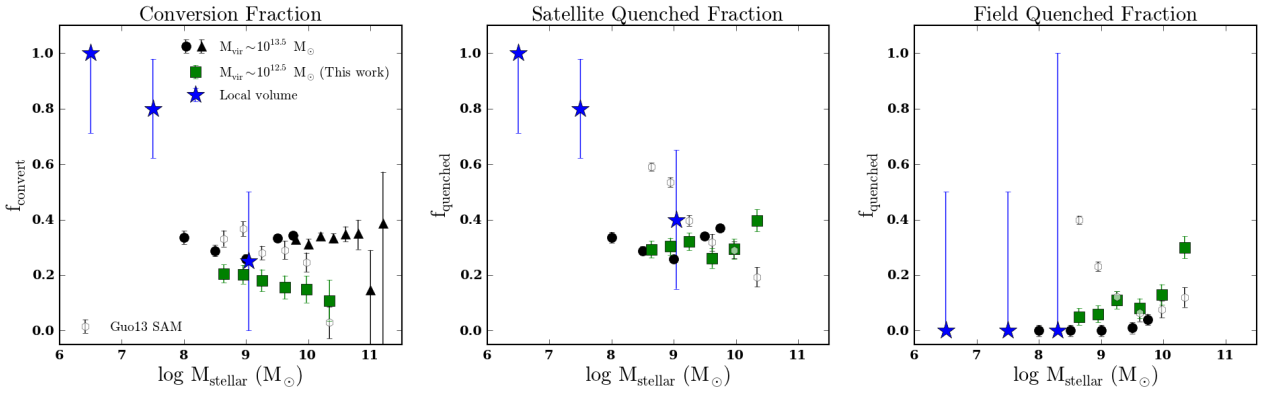

Figure 8. Conversion fractions (left panel), satellite quenched fractions (center panel), and field quenched fractions (right panel) for our sample of Milky Way-like systems ($M_{vir} \sim 10^{12.5}$ $M_\odot$; green squares). For comparison, we show various samples of local galaxies including group-scale systems ($M_{vir} \sim 10^{13.5}$ $M_\odot$, black circles: Geha et al. 2012; Wheeler et al. 2014; black triangles: Wetzel et al. 2013), the Local Group/Local Volume (blue stars) and simulated galaxies from the Guo et al. (2013) SAM (open grey hexagons). At stellar masses greater than 10^8 $M_\odot$, conversion fractions show little to no dependance on satellite stellar mass at fixed host halo mass. At fixed satellite stellar mass, hosts with greater virial masses quench their satellites more effectively. A significantly greater fraction of Local Group satellites are quenched than higher mass satellites, indicating a potential critical mass scale for satellite quenching at $\sim 10^8$ $M_\odot$. The differences between the SAM and the observational data is likely driven by overpredicting the field quenched fraction at these masses. Note that we exclude likely "backsplash galaxies" (i.e. galaxies believed to have previously interacted with their host, namely Cetus) from the Local Field sample.

ficiency. Figure 8 shows our measurements of (*i*) satellite conversion fraction, (*ii*) satellite quenched fraction, and (*iii*) field quenched fraction as function of satellite stellar mass for Milky Way-like hosts (i.e. our "main sample"). For comparison, we include complementary results from Wheeler et al. (2014) and Wetzel et al. (2013) along side corresponding measurements for the Local Group and the Guo et al. (2013) semi-analytic model (SAM). Both the Wheeler et al. (2014) and Wetzel et al. (2013) studies find higher conversion fractions at all stellar masses. This relative increase in quenching efficiency is likely driven by variations in the sample selection that lead to significant differences in the typical halo masses probed. As shown by Wheeler et al. (2014), the typical host in the Geha et al. (2012) sample has a halo mass of $\sim 10^{13.5}$ $M_\odot$, comparable to that of the group catalog employed by Wetzel et al. (2013). Our methodology differs in that we apply isolation criteria so as to restrict our analysis to 10^{12} $M_\odot$ halos. This places our hosts at systematically lower virial masses than the above works, which in turn biases our results towards environments of lower quenching efficiency.

Our work, taken together with the complementary results described above, paints a picture of relatively low satellite quenching efficiency ($\sim$ 30%) that is independent of satellite stellar mass across an impressively broad range in mass ($10^8 < M_\star/M_\odot < 10^{11}$). At stellar masses of $> 10^8$ $M_\odot$, observations of the Local Group are remarkably consistent with these results. Among the massive satellites of the Milky Way and M31, the LMC, SMC, and M33 are star-forming while NGC 205 and M32 are quenched, yielding a quenched fraction of 40% and conversion fraction of roughly 25%. Here, we define objects in the Local Group and surrounding field population as quenched according to their observed atomic gas fractions as reported by McConnachie (2012), such that objects with $M_{HI}/M_\star < 0.1$ are classified as quenched. For the field population surrounding the Local Group, we find that nearly all galaxies are star-forming, where the rare exceptions (e.g. Cetus and Tucana) are likely systems that previously interacted with either the Milky Way or M31 (i.e. "backsplash" or "super-virial" galaxies, Mamon et al. 2004, Wetzel et al. 2014, Garrison-Kimmel et al. in prep). This broadly agrees with our observations of low-mass isolated systems as well as the results of Geha et al. (2012).

While at stellar masses of $> 10^8$ $M_\odot$ the satellite population in the Local Group shows broad agreement with the observed properties of satellites around our sample of Milky Way-like systems, at lower stellar masses Local Group satellites exhibit a dramatically greater quenched fraction and quenching efficiency (see Fig. 8). With one exception, IC10, every satellite galaxy of both the Milky Way and M31 below 10^8 $M_\odot$ is quenched. This dramatic increase in satellite quenching efficiency at low stellar masses ($< 10^8$ $M_\odot$) points towards a potential critical mass scale for satellite quenching, such that environmental quenching is highly efficient for very low-mass satellites.

Observations of systems in the local Universe comparable to the Local Group generally confirm the increased satellite quenching efficiency at low masses. For example, the low-mass ($\sim$ a few $\times 10^6$ $M_\star$) satellites of M81 are universally quenched, with observed star formation rates of $< 10^{-5}$ $M_\odot$ yr^{-1} (Kaisin & Karachentsev 2013). In addition, recent observations of the NGC 4258 group find an overall satellite quenched fraction of $\sim$ 50% at $< 10^8$ $M_\odot$, including some objects with blue rest-frame colors likely to be satellites at stellar masses equal to Fornax and Leo I (Spencer, Loebman & Yoachim 2014). Such observations, however, must be interpreted under the caveat that there is significantly greater uncertainty in determining which objects are satellites and which objects belong to the field in systems beyond the Local Group, where line-of-sight distances are more poorly constrained. Given that the field is

highly dominated by star-forming systems at these masses, sample contamination will strongly bias results to systematically lower quenched fractions.

Altogether, the observational results from our work and others, which constrain the relative impact of self-quenching and environmental quenching at low masses, present a challenge to models of galaxy evolution. Previous studies at higher stellar mass ($> 10^{9.5}$ $M_\odot$) find that modern semi-analytic models overpredict the fraction of quenched satellites (Weinmann et al. 2010; Wang & White 2012). In particular, Kimm et al. (2009) find that while semi-analytic models overestimate the number density of quenched satellites at high masses, the same models are generally able to reproduce the observed quenched fraction in the field, suggesting that conflicts with observations are largely driven by overprediction of the the impact of environmental quenching (i.e. overestimation of the satellite quenching efficiency) at $> 10^{9.5}$ $M_\odot$.

Applying our sample selection criteria to the Guo et al. (2013) semi-analytic model yields a satellite quenched fraction significantly elevated with respect to observations at $< 10^{9.5}$ $M_\odot$.[4] However, the increased number of quenched satellites in the model is largely driven by a corresponding overprediction of quenched field systems. At stellar masses $> 10^{9.5}$ $M_\odot$, where our data overlap with that of Kimm et al. (2009), we similarly find that the model reproduces the field quenched fraction, while at lower masses the Guo et al. (2013) SAM yields an excessive number of quenched centrals. Thus, while the model does overpredict the efficiency of satellite quenching (i.e. $f_{convert}$) at low masses, the effect is subdominant. Below 10^9 $M_\odot$, the observed conversion fractions agree with those in the semi-analytic model to within 50%, while the model overpredicts the quenched fraction of field objects by roughly a factor of 5. Combined with the results of Kimm et al. (2009), we find that modern models primarily fail to accurately describe the physics of feedback (i.e. self-quenching) within low-mass galaxies and the environmental quenching of high-mass galaxies.

5 CONCLUSIONS

In this work, we study the quenching of satellite galaxies in Milky Way-like systems, primarily focusing on the dependence of quenching efficiency on both satellite and host mass. Our principal results are as follows:

- The efficiency of satellite quenching is largely independent of satellite mass over roughly three orders of magnitude in stellar mass, 10^8 $M_\odot < M_\star < 10^{11}$ $M_\odot$. Comparison to the Local Group suggests that satellite quenching efficiency may be significantly greater at yet lower stellar masses ($< 10^8$ $M_\odot$), perhaps indicating a critical mass for satellite quenching.
- Satellite quenching efficiency is well correlated with host halo mass, such that satellites of more massive halos are more likely to be quenched. A model in which satellite quenching only occurs in halos above a given critical halo mass is consistent with (*i*) the observed increase in satellite quenching in systems with two massive satellites (i.e. more massive halos) relative to those with one massive satellite in addition to (*ii*) the higher incidence of quenched satellites around passive hosts relative to their star-forming counterparts with one massive satellite.
- Discrepancies between the observed quenched fractions of low-mass ($< 10^{9.5}$ $M_\odot$) field and satellite galaxies and the predictions of the Guo et al. (2013) semi-analytic model are primarily driven by overly-effective internal processes (i.e. feedback or self-quenching mechanisms) that yield an overabundance of quenched field systems in the models. While the SAM overpredicts the efficiency of satellite quenching at low masses, the excess number of quenched satellites in the model is largely a product of the overabundance of quenched field systems. In contrast, at higher masses ($> 10^{9.5}$ $M_\odot$), SAMs are generally able to reproduce the star-forming properties of field (or central) galaxies, while they instead fail to accurately model the environmental quenching mechanisms, thereby overpredicting the number of quenched satellites at $> 10^{9.5}$ $M_\odot$.

[4] In the SAM, we consider an object "quenched" if it has a SSFR less than 10^{-11} yr^{-1}.

ACKNOWLEDGMENTS

We thank Marla Geha, Andrew Wetzel and their collaborators for kindly suppling their observational results in tabular form, as well as for productive discussions. CW and JSB recognize support from NSF grants AST-1009973 and AST-1009999.

Funding for the SDSS and SDSS-II has been provided by the Alfred P. Sloan Foundation, the Participating Institutions, the National Science Foundation, the U.S. Department of Energy, the National Aeronautics and Space Administration, the Japanese Monbukagakusho, the Max Planck Society, and the Higher Education Funding Council for England. The SDSS Web Site is http://www.sdss.org/.

The SDSS is managed by the Astrophysical Research Consortium for the Participating Institutions. The Participating Institutions are the American Museum of Natural History, Astrophysical Institute Potsdam, University of Basel, University of Cambridge, Case Western Reserve University, University of Chicago, Drexel University, Fermilab, the Institute for Advanced Study, the Japan Participation Group, Johns Hopkins University, the Joint Institute for Nuclear Astrophysics, the Kavli Institute for Particle Astrophysics and Cosmology, the Korean Scientist Group, the Chinese Academy of Sciences (LAMOST), Los Alamos National Laboratory, the Max-Planck-Institute for Astronomy (MPIA), the Max-Planck-Institute for Astrophysics (MPA), New Mexico State University, Ohio State University, University of Pittsburgh, University of Portsmouth, Princeton University, the United States Naval Observatory, and the University of Washington.

Support for this work was provided by NASA through Hubble Fellowship grant 51316.01 awarded by the Space Telescope Science Institute, which is operated by the Association of Universities for Research in Astronomy, Inc., for NASA, under contract NAS 5-26555.

REFERENCES

Abazajian K. N. et al., 2009, ApJS, 182, 543
Baldry I. K., Balogh M. L., Bower R. G., Glazebrook K., Nichol R. C., Bamford S. P., Budavari T., 2006, MNRAS, 373, 469
Baldry I. K., Glazebrook K., Brinkmann J., Ivezić Ž., Lupton R. H., Nichol R. C., Szalay A. S., 2004, ApJ, 600, 681
Balogh M. L., Baldry I. K., Nichol R., Miller C., Bower R., Glazebrook K., 2004, ApJ, 615, L101
Balogh M. L., Morris S. L., 2000, MNRAS, 318, 703
Balogh M. L., Navarro J. F., Morris S. L., 2000, ApJ, 540, 113
Behroozi P. S., Wechsler R. H., Conroy C., 2012, ArXiv e-prints
Berrier J. C., Bullock J. S., Barton E. J., Guenther H. D., Zentner A. R., Wechsler R. H., 2006, ApJ, 652, 56
Bigiel F., Leroy A., Walter F., Brinks E., de Blok W. J. G., Madore B., Thornley M. D., 2008, AJ, 136, 2846
Binney J., 1977, ApJ, 215, 483
Birnboim Y., Dekel A., 2003, MNRAS, 345, 349
Blanton M. R. et al., 2005, AJ, 129, 2562
Boselli A., Cortese L., Boquien M., Boissier S., Catinella B., Lagos C., Saintonge A., 2014, A&A, 564, A66
Boylan-Kolchin M., Bullock J. S., Kaplinghat M., 2011, MNRAS, 415, L40
Boylan-Kolchin M., Bullock J. S., Kaplinghat M., 2012, MNRAS, 422, 1203
Boylan-Kolchin M., Bullock J. S., Sohn S. T., Besla G., van der Marel R. P., 2013, ApJ, 768, 140
Boylan-Kolchin M., Springel V., White S. D. M., Jenkins A., Lemson G., 2009, MNRAS, 398, 1150
Brinchmann J., Charlot S., White S. D. M., Tremonti C., Kauffmann G., Heckman T., Brinkmann J., 2004, MNRAS, 351, 1151
Conroy C. et al., 2007, ApJ, 654, 153
Conroy C., Wechsler R. H., Kravtsov A. V., 2006, ApJ, 647, 201
Cooper M. C. et al., 2010a, MNRAS, 409, 337
Cooper M. C., Gallazzi A., Newman J. A., Yan R., 2010b, MNRAS, 402, 1942
Cooper M. C. et al., 2007, MNRAS, 376, 1445
Cooper M. C. et al., 2006, MNRAS, 370, 198
Cooper M. C. et al., 2008, MNRAS, 383, 1058
Crain R. A. et al., 2009, MNRAS, 399, 1773
Davé R., Oppenheimer B. D., Finlator K., 2011, MNRAS, 415, 11
Davis M., Geller M. J., 1976, ApJ, 208, 13
De Lucia G., Weinmann S., Poggianti B. M., Aragón-Salamanca A., Zaritsky D., 2012, MNRAS, 423, 1277
Deason A. J. et al., 2012, MNRAS, 425, 2840
Dressler A., 1980, ApJ, 236, 351
Farouki R., Shapiro S. L., 1981, ApJ, 243, 32
Gabor J. M., Davé R., 2014, ArXiv e-prints
Garrison-Kimmel S., Boylan-Kolchin M., Bullock J. S., Kirby E. N., 2014, ArXiv e-prints
Geha M., Blanton M. R., Masjedi M., West A. A., 2006, ApJ, 653, 240
Geha M., Blanton M. R., Yan R., Tinker J. L., 2012, ApJ, 757, 85
Gunn J. E., Gott, III J. R., 1972, ApJ, 176, 1
Guo Q., White S., Angulo R. E., Henriques B., Lemson G., Boylan-Kolchin M., Thomas P., Short C., 2013, MNRAS, 428, 1351
Guo Q. et al., 2011, MNRAS, 413, 101
Hearin A. P., Watson D. F., van den Bosch F. C., 2014, ArXiv e-prints
Hogg D. W. et al., 2004, ApJ, 601, L29
Kaisin S. S., Karachentsev I. D., 2013, Astrophysics, 56, 305
Kauffmann G. et al., 2003, MNRAS, 341, 54
Kauffmann G., Li C., Zhang W., Weinmann S., 2013, MNRAS, 430, 1447
Kennicutt, Jr. R. C. et al., 2007, ApJ, 671, 333
Kereš D., Katz N., Fardal M., Davé R., Weinberg D. H., 2009, MNRAS, 395, 160
Kereš D., Katz N., Weinberg D. H., Davé R., 2005, MNRAS, 363, 2
Kimm T. et al., 2009, MNRAS, 394, 1131
Komatsu E. et al., 2011, ApJS, 192, 18
Larson R. B., Tinsley B. M., Caldwell C. N., 1980, ApJ, 237, 692
Leroy A. K., Walter F., Brinks E., Bigiel F., de Blok W. J. G., Madore B., Thornley M. D., 2008, AJ, 136, 2782
Lewis I. et al., 2002, MNRAS, 334, 673
Mamon G. A., Sanchis T., Salvador-Solé E., Solanes J. M., 2004, A&A, 414, 445
Mandelbaum R., Seljak U., Kauffmann G., Hirata C. M., Brinkmann J., 2006, MNRAS, 368, 715
McConnachie A. W., 2012, AJ, 144, 4
McGaugh S. S., 2012, AJ, 143, 40
Miller S. H., Bundy K., Sullivan M., Ellis R. S., Treu T., 2011, ApJ, 741, 115
Miller S. H., Ellis R. S., Newman A. B., Benson A., 2014, ApJ, 782, 115
Moore B., Katz N., Lake G., Dressler A., Oemler A., 1996, Nature, 379, 613
Moster B. P., Naab T., White S. D. M., 2013, MNRAS, 428, 3121
Moster B. P., Somerville R. S., Maulbetsch C., van den Bosch F. C., Macciò A. V., Naab T., Oser L., 2010, ApJ, 710, 903
Pasquali A., Gallazzi A., Fontanot F., van den Bosch F. C., De Lucia G., Mo H. J., Yang X., 2010, MNRAS, 407, 937
Peng Y.-j. et al., 2010, ApJ, 721, 193
Peng Y.-j., Lilly S. J., Renzini A., Carollo M., 2012, ApJ, 757, 4
Phillips J. I., Wheeler C., Boylan-Kolchin M., Bullock J. S., Cooper M. C., Tollerud E. J., 2014, MNRAS, 437, 1930
Postman M. et al., 2005, ApJ, 623, 721
Quilis V., Moore B., Bower R., 2000, Science, 288, 1617
Rees M. J., Ostriker J. P., 1977, MNRAS, 179, 541
Saintonge A. et al., 2011, MNRAS, 415, 32
Salim S. et al., 2007, ApJS, 173, 267
Schiminovich D. et al., 2010, MNRAS, 408, 919
Skillman E. D., Côté S., Miller B. W., 2003, AJ, 125, 593
Spencer M., Loebman S., Yoachim P., 2014, ArXiv e-prints
Stewart K. R., Kaufmann T., Bullock J. S., Barton E. J., Maller A. H., Diemand J., Wadsley J., 2011, ApJ, 735, L1
Strateva I. et al., 2001, AJ, 122, 1861
Tollerud E. J., Boylan-Kolchin M., Barton E. J., Bullock J. S., Trinh C. Q., 2011, ApJ, 738, 102

van den Bosch F. C., Aquino D., Yang X., Mo H. J., Pasquali A., McIntosh D. H., Weinmann S. M., Kang X., 2008, MNRAS, 387, 79
van der Marel R. P., Fardal M., Besla G., Beaton R. L., Sohn S. T., Anderson J., Brown T., Guhathakurta P., 2012, ApJ, 753, 8
Wang W., White S. D. M., 2012, MNRAS, 424, 2574
Weinmann S. M., Kauffmann G., von der Linden A., De Lucia G., 2010, MNRAS, 406, 2249
Weinmann S. M., Pasquali A., Oppenheimer B. D., Finlator K., Mendel J. T., Crain R. A., Macciò A. V., 2012, MNRAS, 426, 2797
Weinmann S. M., van den Bosch F. C., Yang X., Mo H. J., 2006, MNRAS, 366, 2
Wetzel A. R., Tinker J. L., Conroy C., Bosch F. C. v. d., 2014, MNRAS, 439, 2687
Wetzel A. R., Tinker J. L., Conroy C., van den Bosch F. C., 2013, MNRAS, 432, 336
Wheeler C., Phillips J. I., Cooper M. C., Boylan-Kolchin M., Bullock J. S., 2014, ArXiv e-prints
Wong T., Blitz L., 2002, ApJ, 569, 157
Woo J. et al., 2013, MNRAS, 428, 3306
Yang X., Mo H. J., van den Bosch F. C., Jing Y. P., 2005, MNRAS, 356, 1293
Yang X., Mo H. J., van den Bosch F. C., Pasquali A., Li C., Barden M., 2007, ApJ, 671, 153
York D. G. et al., 2000, AJ, 120, 1579